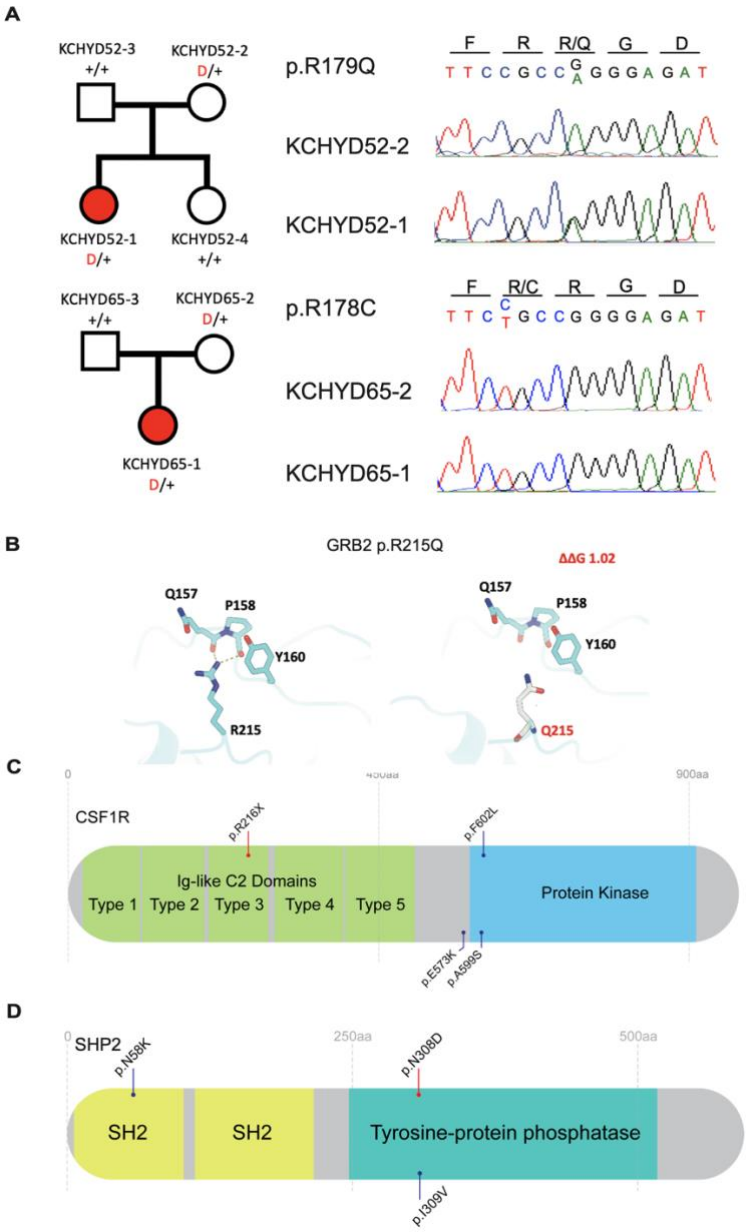

Supplementary Figure 1: Protein-protein interaction modeling of GRB2 variant p.R215Q. (A) Pedigrees and Sanger sequencing electropherograms depicting *GRB2* mutations in genomic DNA from congenital hydrocephalus proband KCHYD52-1 and KCHYD65-1. (B) Deleterious missense variant p.R215Q (DDG 1.02) is predicted by Alpha-Fold as detrimental to *GRB2* structure and function to loss of multiple hydrogen bonds that normally constrain loop region flexibility, thus indirectly destabilizing the adjacent constitutive GRB2 phosphorylation site Y160. (C) Schematic diagrams of CSF1R protein and (D) SHP2 protein domains showing variant locations. Variants from our CH cohort are indicated in red, and variants from GMKF database are in blue. Axis depicts protein length (aa, in gray).

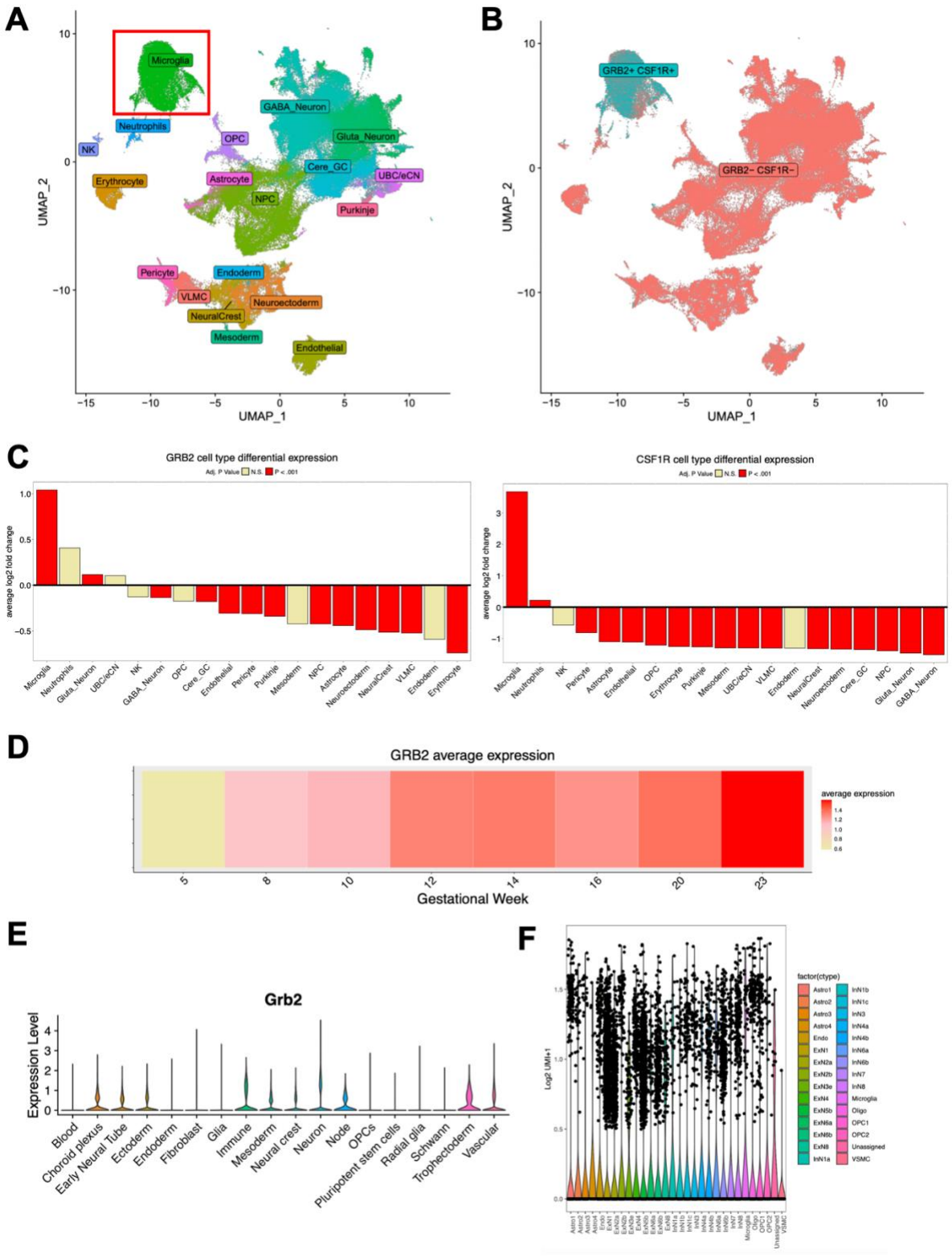

Supplementary Figure 2: *GRB2* and *CSF1R* expression profiling in a single-cell atlas of early developing human brain development. (A) UMAP plot colored by main cell type. Neural progenitor cell (NPC), common glutamatergic neuron (Gluta_Neuron), Cerebellar granule cell (Cere_GC), unipolar brush cell/excitatory cerebellar nuclei (UBC/eCN), common GABAnergic neuron (GABA_Neuron), oligodendrocyte precursor cell (OPC), and vascular leptomeningeal cells (VLMC). (B) UMAP plot identifying *GRB2*+ *CSF1R*+ cells. (C) *GRB2* and *CSF1R* differential expression across cell types. (D) Temporal expression of *GRB2* between gestational weeks 5-23. (E) *GRB2* expression in cell types of prenatal human brain transcriptomics atlas. (F) *GRB2* expression in the adult human brain single-nucleus RNA sequencing data.

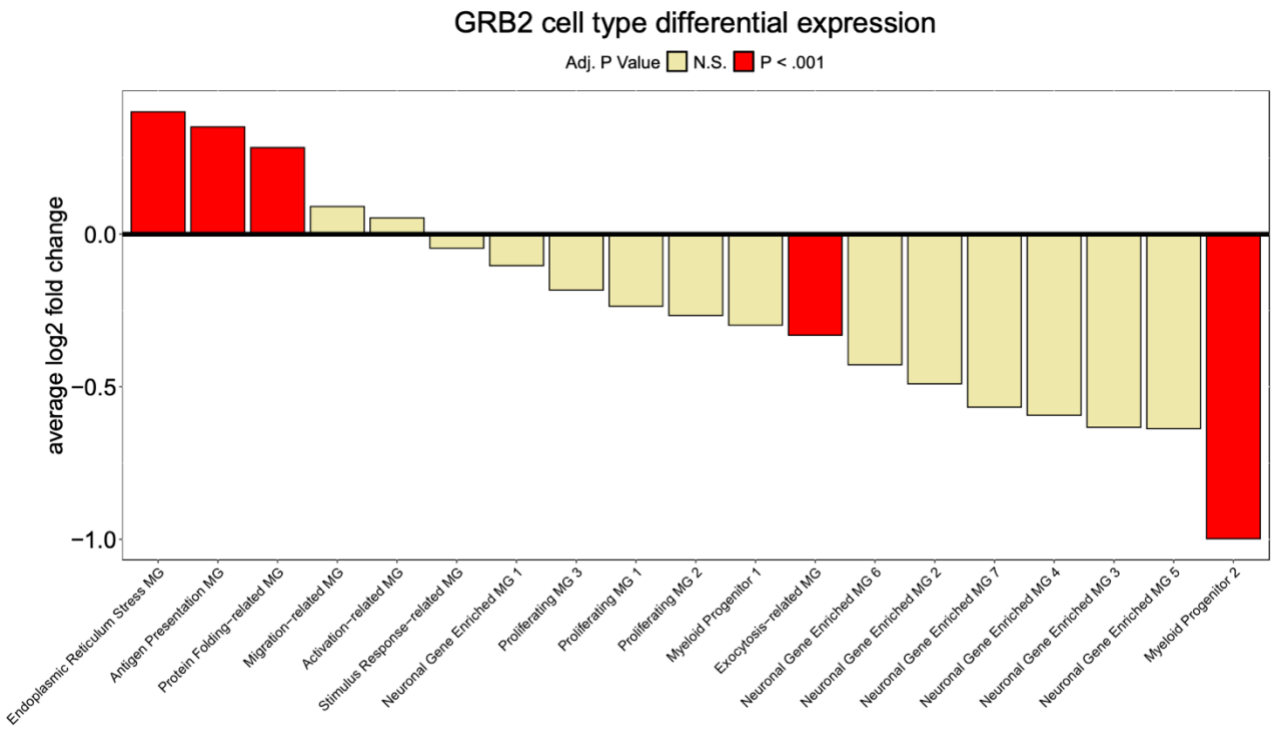

Supplementary Figure 3: *GRB2* differential expression across microglial subclusters. Clusters labeled by biological function based on top differentially expressed genes.

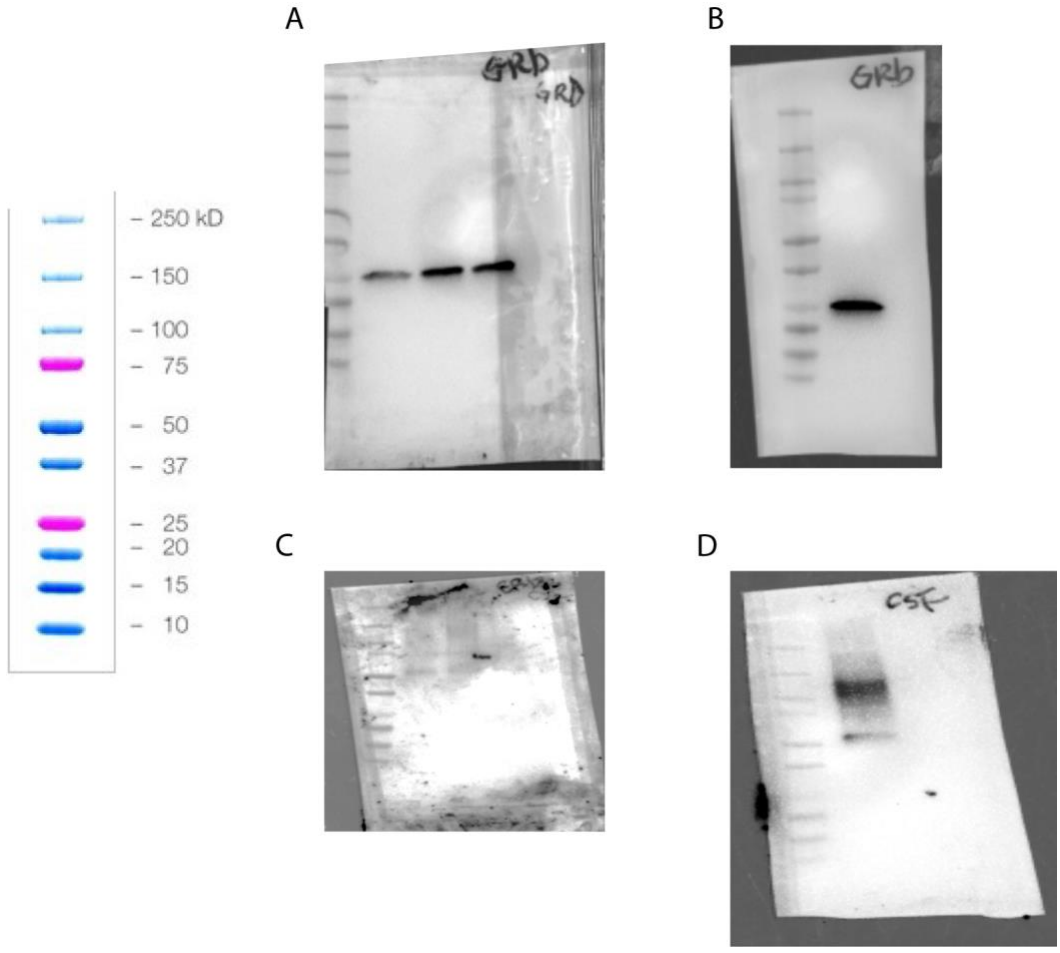

Supplementary Figure 4: Source data. A) Source blot corresponding to Figure 2G, top lane. B) Source blot corresponding to Figure 2G, third lane down from top. C) Source blot corresponding to Figure 2G, second lane down from top. D) Source blot corresponding to Figure 2G, fourth lane down from top.

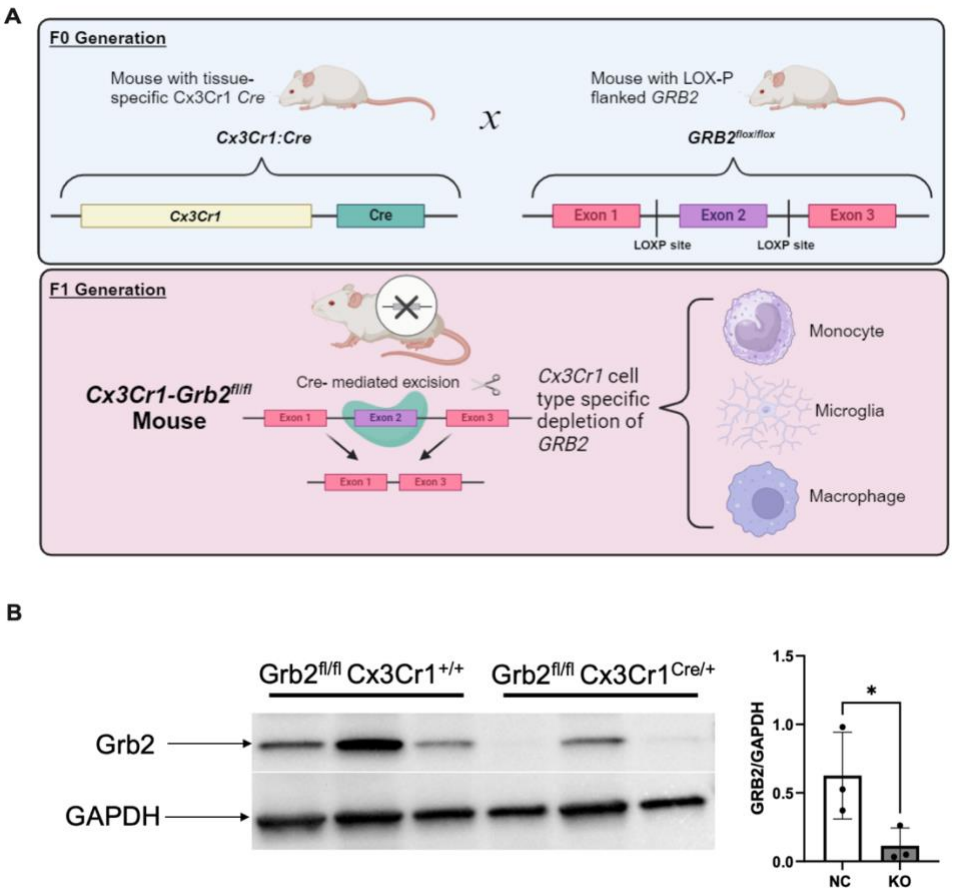

Supplementary Figure 5: Methodology and confirmation of microglia-specific knockout of GRB2 in mouse model. (A) Schematic of cross between *Cx$_3$Cr1*:Cre mice and conditional *Grb2$^{fl/fl}$* mice to generate progeny *Cx$_3$Cr1-Grb2$^{fl/fl}$* mice with functional *Grb2* deletion from all mononuclear phagocytes, including microglia. (B) Immunoblot for Cx3Cr1+ peritoneal macrophages of Grb2$^{fl/fl}$ Cx3Cr1$^{+/+}$ mice (negative control, NC) and Grb2$^{fl/fl}$ Cx3Cr1$^{cre/+}$ mice (KO), done with an anti-Grb2 antibody and an anti-GAPDH antibody as a control. Quantification of protein expression normalized to the level of GAPDH; means ± SEM, n = 3 samples per group, *P < 0.05.

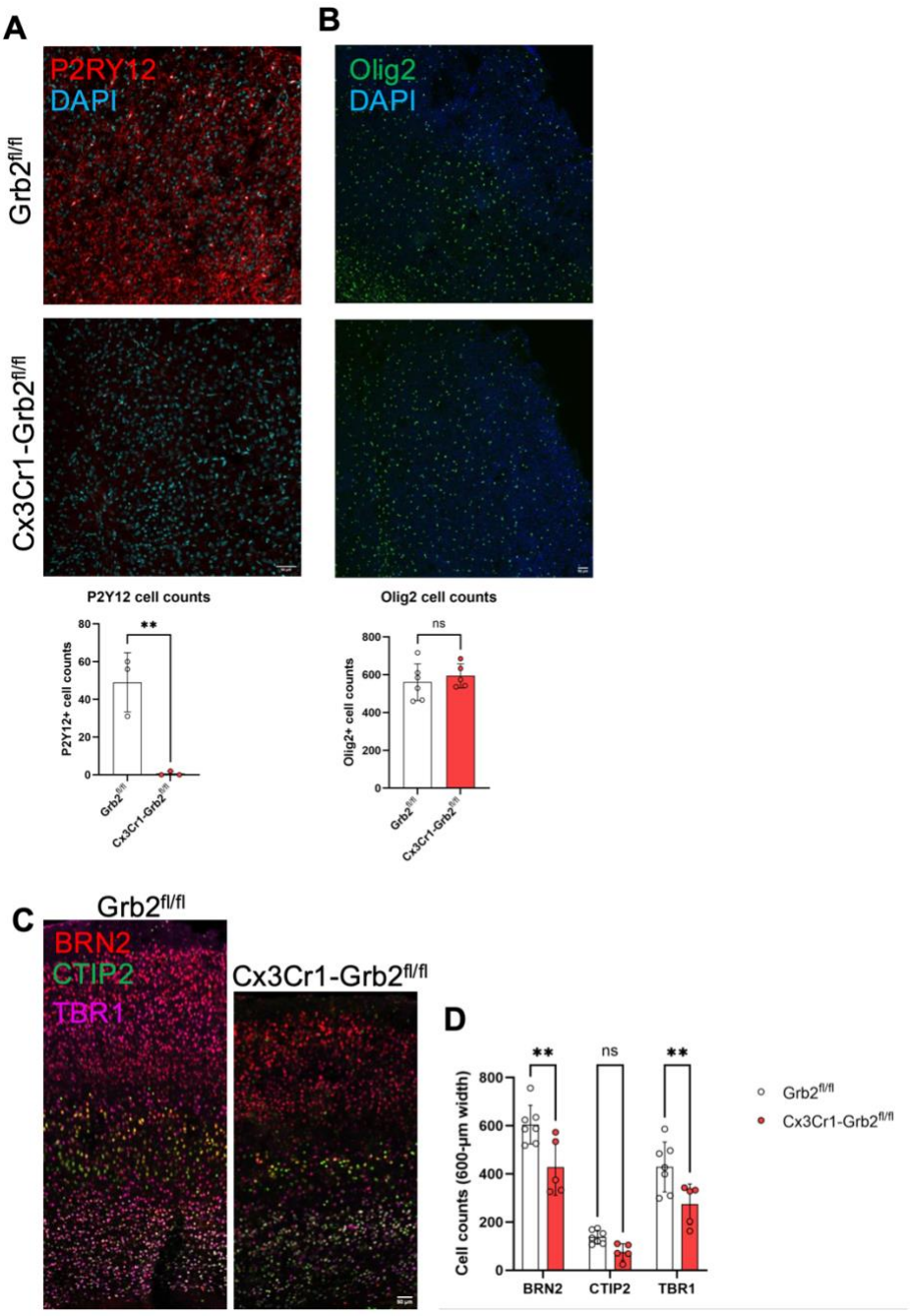

Supplementary Figure 6: Characterization of microglia-specific knockout of GRB2 in the mouse brain. (A–B) Representative immunostaining of P2Y12 (A, microglia marker) and Olig2 (B, oligodendrocyte marker) in brains of *Grb2*$^{fl/fl}$ and *Cx3cr1-Grb2*$^{fl/fl}$ mice. Quantification of P2RY12^{+} cells (A), Olig2^{+} cells (B), and GFAP fluorescence intensity (C) is shown below the respective images. *n* = 3 (A), *n* = 5–6 (B), *n* = 5 (C); unpaired Student's *t*-test. (D) Immunostaining of BRN2 (layer II–III cortical neurons), BCL11B/CTIP2 (layer V cortical neurons), and TBR1 (layer VI cortical neurons) in cortices of *Grb2*$^{fl/fl}$ and *Cx3cr1-Grb2*$^{fl/fl}$ mice. (E) Quantification of cell numbers from panel D. *n* = 5–7; two-way ANOVA followed by Bonferroni's multiple comparisons test. Scale bar: 50 µm.

Supplementary Table 1. Summary of Human and Mouse Evidence Linking CSF1R and PTPN11 (SHP2) Mutations to Hydrocephalus and/or Ventriculomegaly.

Gene	Species	Type of Study / Model	Phenotype Description (Hydrocephalus/Ventriculomegaly)	OMIM	Citation
CSF1R	**Human**	Case report (n=1)	Adult-onset leukoencephalopathy (HDLS) with striking ventricular enlargement misdiagnosed as NPH. **Variant:** Heterozygous mutation c.2552T>C (p.L851P)	221820	Wang *et al.* 2019 (PMID:31093799)
		Case series (n=7)	Recessive CSF1R mutations (BANDDOS): congenital hydrocephalus with ventriculomegaly, callosal agenesis, and cerebellar hypoplasia. **Variants:** c.395C>T (p.Pro132Leu), c.1441C>T (p.Gln481*), c.1859119G>A (p.Ser620delins40), c.1879_1881del (p.Lys627del), c.1969þ115_1969þ116del (p.Pro658Serfs*24)	618476 224300 265990	Guo *et al.* 2019 (PMID:30982609)
		Case series (n=2)	Ventriculomegaly with callosal agenesis and pontocerebellar hypoplasia due to near-complete absence of microglia. **Variants:** c.1754-1G>C, c.1929C>A (p.His643Gln)	618476	Oosterhof *et al.* 2019 (PMID:30982608)
		Case series (n=2)	Dandy-Walker malformation, occipital ventriculomegaly (colpocephaly), callosal agenesis, periventricular calcifications. **Variant:** c.1620T>A (p.Tyr540*)	220200	Monies *et al.* 2017 (PMID:28383543)
		Case report (n=1)	Childhood-onset neurodegeneration with cerebral atrophy, ex-vacuo ventricular dilatation, and periventricular white matter abnormalities; confirmed biallelic hypomorphic mutation (p.T833M). **Variants:** Chr5:149435645G > A /c.2498C > T /p.(Thr833Met) /rs780804532	164770	Tamhankar *et al.* 2020 (PMID:32464672)
		Case series (n=7)	Ventricular enlargement (lateral ventricles), thinning of corpus callosum, white matter loss with frontal predominance, progressive cerebral atrophy. **Variants:** c.2294G.A/p.G765D, c.2342C.A/p.A781E, c.2470C.T/p.P824S, c.244211G.T, c.2060_2061insT/p.S688EfsX13, c.2381T.C/p. I794T	164770	Konno *et al.* 2014 (doi:10.1212/WNL.0000000000000046)
		Cohort study (n=26)	Dilation of lateral ventricles, thinning of the corpus callosum, white matter lesions, and calcifications in white matter.	164770	Konno *et al.* 2017 (doi:10. 1111/ene.13125)
		Observational study (n=1)	Misdiagnosed NPH; later found to have CSF1R mutation (HDLS).	164770	Rademakers *et al.* 2012 (doi:10.1038/ng.1027)
		Cohort Study (n=13)	Brain abnormalities included white matter changes, calcifications, agenesis of corpus callosum, ventriculomegaly, Dandy-Walker complex, and cortical abnormalities.	618476 220200 221820	Dulski *et al.* 2023 (PMID:37349768)
		Case report (n=1)	Brain MRI disclosed frontoparietal lobe atrophy and ventricular dilatation with high-intensity lesions in the cerebral deep white matter **Variant:** de novo K793T mutation	221820	Kondo *et al.* 2013 (PMID:23411710)

		Case report (n=1)	Brain MRI showed cerebral atrophy, enlarged lateral ventricles, thinning of the corpus callosum, and leukoencephalopathy in the frontal-parietal lobes. **Variant:** c.2330G>A/p.R777Q	221820	Yokote *et al.* 2020 (PMID:32435043)
		Familial case series (n=1)	Severe diffuse white matter atrophy and dilation of lateral and third ventricles. Hypoperfusion of cerebral cortices. **Variant:** heterozygous c.653C>Y	221820	Riku *et al.* 2014 (PMID: 25383640)
		Case report (n=1)	Progressive confluent periventricular white matter lesions and enlarged lateral ventricles. **Splicing mutation**: c.1858+1G>T (exon 13 skipping)	221820	Yang *et al.* 2019 (doi: 10.3389/fgene.2019.00491)
		Case series (n=3)	Global atrophy and enlarged ventricles. **Variant:** c.2342C>T (p.A781V), exon 18	221820	Battisti *et al.* 2014 (PMID:24532199)
		Case report (n=1)	Multifocal leukoencephalopathy, thinning of corpus callosum, ventriculomegaly, parieto-occipital involvement. **Variant:** c.2539G>A (p.Glu847Lys), exon 19	221820	Di Donato *et al.* 2015 (PMID:26401554)
		Case report (n=2)	Diffuse brain atrophy, ventricular enlargement, bilateral white matter changes. **Variant:** c.2264T>C (p.L755P)	221820	Du *et al.* 2021 (PMID:30617447)
		Case report (n=1)	Severe cerebral atrophy and lateral/third ventricular enlargement. **Variant:** c.2442+2T>C, exon 18	221820	Kawakami *et al.* 2016 (PMID:27423618)
		Case series (n=1)	Frontal atrophy, periventricular white matter lesions, and lateral ventricle dilation. **Variant:** c.2381T>C (p.I794T)	221820	Kim *et al.* 2017 (PMID:29044417)
		Case report (n=1)	Confluent white matter lesions in frontoparietal lobes, ventriculomegaly. **Variant:** c.2539G>A (p.E847K), exon 19	221820	Kim *et al.* 2019 (PMID:30853829)
		Case report (n=1)	Frontal-predominant diffuse leukoencephalopathy, thinning of anterior corpus callosum, ventriculomegaly. **Variant:** c.2350G>A (p.V784M), exon 18	221820	La Piana *et al.* 2014 (PMID:25012610)
		Case report (n=1)	Severe corpus callosum thinning and ventricular dilation. Persistent diffusion-restricted lesions. **Variant:** c.2319+1C>A, intron 16	221820	Leng *et. al*. 2019 (PMID:31632577)
		Case report (n=1)	Diffuse frontal white matter atrophy and progressive ventriculomegaly **Variant:** c.2473G>A (p.E825K), exon 19	221820	Lynch *et al.* 2016 (PMID:25935893
		Case series (n=6)	Periventricular and subcortical WM lesions, ventriculomegaly, callosal thinning. **Variants:** c.2546_2548delTCT, c.2381T>C (p.I794T), c.2563C>A	221820	Mao *et. al*. 2020 (PMID:31705326)
		Case report (n=1)	Frontal and occipital white matter hyperintensities, enlarged frontal horns, diffuse atrophy. **Variant:** c.2345G>A (p.R782H), exon 18	221820	Nicholson *et al.* 2013 (PMID: 23408870)
		Case report (n=1)	Mild atrophy, periventricular calcifications, ventriculomegaly, and gliosis. **Variant:** c.2467C>T (p.Ala823Val), exon 19	221820	Terasawa *et al.* 2013 (PMID:24094860)

		Case report (n=1)	Diffuse cerebral atrophy with frontal predominance and lateral/third ventricle enlargement. **Variant:** c.2552T>C (p.L851P), exon 19	221820	Wang M., Zhang, X. 2019 (PMID:31093799)
		Familial case series (n=1)	Global atrophy, enlarged ventricles, posterior callosal thinning. **Variant:** c.2342C>T (p.A781V), exon 18	221820	Ahmed *et al.* 2013 (PMID: 23816250)
		Case series (n=1)	Enlarged ventricles with frontal-predominant WM lesions. **Variant:** c.1990G>A (novel heterozygous mutation), exon 15	221820	Eichler *et al.* 2016 (PMID: 27190017)
	Mouse	KI	*Csf1r*$^{E631K/E631K}$ homozygotes: absent microglia, severe ventriculomegaly, callosal hypoplasia, hydrocephalus, perinatal lethality.	-	Stables *et al.* 2022 (PMID: 35333324)
		Constitutive KO	*Csf1r*$^{-/-}$ mice: lethal hydrocephalus with ventricular dilation and cortical thinning.	-	Erblich *et al.* 2011 (PMID:22046273)
		Heterozygous KO	*Csf1r*$^{+/-}$ adult mice: ventriculomegaly, callosal thinning, white matter degeneration.	-	Chitu *et al.* 2015 (PMID:25497733)
		KO	Enlarged ventricles, reduced cortex, global brain size reduction.	-	Nandi *et al.* 2012 (doi:10.1016/j.ydbio.2012.03.026)
***PTPN11* (SHP2)**	**Human**	Case report (n=1)	Noonan syndrome with obstructive tetraventricular hydrocephalus due to a fourth ventricle outlet obstruction (diverticulum of Luschka); resolved after endoscopic ETV.	163950	Spennato *et al.* 2019 (PMID: 30822582)
		Case series (prenatal; n=1)	Prenatal diagnosis of Noonan syndrome with external hydrocephalus (enlarged subarachnoid spaces) from 19 weeks gestation. **Variant:** c.124A>G, p.Thr42Ala; chr12-112884189 A>G, NM_002834.5, rs397507501	163950	Elekes *et al.* 2025 (doi:10.3390/jcm14113973)
		Case report (prenatal, n=1)	Fetal Noonan syndrome: external hydrocephalus on MRI. Variant: *PTPN11*(p.Asn308Ser)	163950	Mastromoro *et al.*, 2021 (PMID:34075583)
	Mouse	KI	*Ptpn11*^{E76K} pan-neuronal knock-in: communicating hydrocephalus via ependymal/ciliary dysfunction; rescued by SHP2 C459S.	-	Zheng *et al.* 2018 (PMID: 29559584)